Combined Source and Vortex Panel Method Analysis

by
Cameron Dix

December 8, 2021

Abstract

Understanding pressure distributions on aerodynamic bodies is critical in aerodynamic design. Numerical panel methods are used to model the pressure acting on a semi-infinite body at low speeds. Panel methods show that the pressure distribution is entirely dependent on the geometry of the body and can be modeled by combining elementary flows to produce dividing flows that follow the shape of the body. By placing source sheets around the surface of the body a non-lifting pressure distribution is found. Placing vortex flows on the surface of the body adds lift to the analysis but is sensitive to geometry. The most accurate method to predict the pressure and lift is found by combining source and vortex flows around the surface of the body. The method is implemented in Python and tested on both the NACA 0012 and NACA 2412 airfoils. The results are very accurate when compared to experimental data at low angles of attack.

1 Introduction

Understanding the pressure distribution on aerodynamic bodies is critical in aerodynamic design. Numerical panel methods are a quick tool to determine the pressure distribution on semi-infinite bodies at low speeds [1]. The common formulations of such methods are based on source panel and vortex panel methods. A combination of the two methods results in quick and accurate estimations of lift. A source vortex panel method will briefly be formulated, and the results will be discussed and compared with experimental data.

2 Formulation

The crux of the panel methods is that there is a direct solution to the combination of elementary flows that create dividing streamlines that fit the shape of the body. Panel methods are entirely geometry based. These methods require decomposing the profile of the body into linear segments referred to as panels, as shown in Figure 1. The end points of each panel are called the boundary points and are denoted by a capital X and Y coordinate. The midpoint of each panel is called the control point and is denoted by a lowercase x and y coordinate. The length of each panel is denoted as s. The body is at an angle of attack α relative to a low-speed incompressible freestream flow V_∞. This formulation requires that the panels be created in a clockwise orientation for the angles to be correct. The counterclockwise angle of the panel relative to the x-axis is defined as [1]

$$\phi = \tan^{-1}\left(\frac{\Delta y}{\Delta x}\right) \tag{1}$$

where ϕ is the angle of the panel, Δx is the change in x from the end to start point of the panel, and Δy is the change in y from the end to start point of the panel. The counterclockwise angle between the panel normal and the freestream is [1]

$$\beta = \phi + 90° - \alpha \tag{2}$$

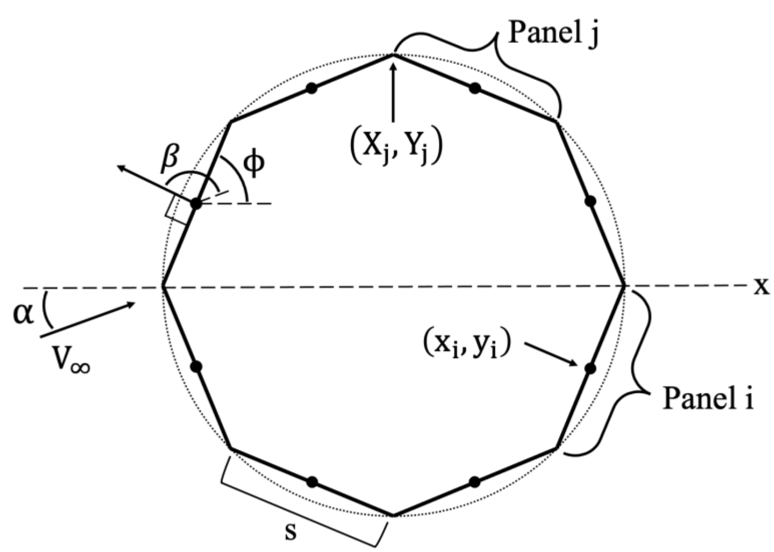

Figure 1: Cylinder decomposed into panels and control points.

2.1 Source Panel Method

The basis of the source panel method is that an infinite number of source flows, of equal strength, are placed along a panel to create a source sheet or source panel. The combination of source panels for each panel on the body produces dividing freestreams that fit the body. Each source sheet induces a velocity potential to all other panels. Knowing that the velocity cannot pass, the normal velocity is zero. A system of equation is formed from the normal velocity equation [1]

$$V_{n,i} = V_{\infty}\cos(\beta_i) + \frac{\lambda_i}{2} + \sum_{\substack{j=1 \\ (j\neq i)}}^{N} \frac{\lambda_j\, I_{i,j}}{2\pi} = 0 \tag{3}$$

where λ is the source strength of the panel i or j, and $I_{i,j}$ is the normal velocity geometric integral of panel i relative to panel j. The integral is simplified as [1]

$$I_{i,j} = \frac{C}{2}\ln\left(\frac{s_j^2 + 2As_j + B}{B}\right) + \frac{D - AC}{E}\left(\tan^{-1}\frac{s_j + A}{E} - \tan^{-1}\frac{A}{E}\right) \tag{4}$$

where

$$A = -(x_i - X_j)\cos\phi_j - (y_i - Y_j)\sin\phi_j$$
$$B = (x_i - X_j)^2 + (y_i - Y_j)^2$$
$$C = \sin(\phi_i - \phi_j)$$
$$D = -(y_i - Y_j)\cos\phi_i - (x_i - X_j)\sin\phi_i$$
$$E = \sqrt{B - A^2}$$

Equations 3 and 4 create the following system in matrix form

$$\begin{bmatrix} \pi & I_{1,2} & \cdots & I_{1,N} \\ I_{2,1} & \pi & \cdots & I_{2,N} \\ \vdots & \vdots & \ddots & \vdots \\ I_{N,1} & I_{N,2} & \cdots & \pi \end{bmatrix} \begin{bmatrix} \lambda_1 \\ \lambda_2 \\ \vdots \\ \lambda_N \end{bmatrix} = \begin{bmatrix} -V_{\infty}2\pi\cos(\beta_1) \\ -V_{\infty}2\pi\cos(\beta_2) \\ \vdots \\ -V_{\infty}2\pi\cos(\beta_N) \end{bmatrix}$$

The source panel strengths are then used to find the tangential velocity at each panel using [1]

$$V_{t,i} = V_{\infty}\sin(\beta_i) + \sum_{\substack{j=1 \\ (j\neq 1)}}^{N} \frac{\lambda_j\, J_{i,j}}{2\pi} \tag{5}$$

where $V_{t,i}$ is the tangential velocity at panel i, and $J_{i,j}$ is the tangential velocity geometric integral of panel i relative to panel j. $J_{i,j}$ is evaluated like $I_{i,j}$ where

$$C = -\cos(\phi_i - \phi_j)$$
$$D = (y_i - Y_j)\sin\phi_i + (x_i - X_j)\cos\phi_i$$

The tangential velocity at each panel is used to find the pressure coefficients using the relationship [1]

$$c_{p,i} = 1 - \left(\frac{V_i}{V_\infty}\right)^2 \tag{6}$$

where $c_{p,i}$ is the pressure coefficient normal to the control point of panel i. The accuracy of the numerical source panel method can be checked by comparing how close the sum of the source strengths is equal to zero [1]

$$\sum_{j=1}^{n} \lambda_j\, s_j = 0 \tag{7}$$

This check validates the method because the body cannot add or subtract mass from the flow, hence the sum of the source strengths must be zero. The limitations of the source panel method are that it always produces zero lift because the circulation from the sources is zero.

2.2 Vortex Panel Method

The vortex panel method follows the same methodology as the source panel method except replaces the source flows with vortex flows. The vortex panel method is used to produce a pressure distribution that creates circulation and to predict lift. The vortex panel method starts with a similar normal velocity equation [1]

$$V_{n,i} = V_\infty \cos(\beta_i) - \sum_{\substack{j=1 \\ (j\neq i)}}^{N} \frac{\gamma_j\, K_{i,j}}{2\pi} = 0 \tag{8}$$

where γ is the vortex strength of each panel, and $K_{i,j}$ is the normal velocity geometric integral of panel i relative to panel j. Mathematically $K_{i,j}$ is equal to $J_{i,j}$. Equation 8 in its current form does not ensure smooth flow at the trailing edge. The Kutta condition must be applied by making the vortex strengths zero at the trailing edge [1]

$$\gamma_i + \gamma_{i+1} = 0 \tag{9}$$

Equation 9 replaces an equation created by Equation 8. Choose to replace the last panel at the trailing edge such that the system of equations in matrix form is

$$\begin{bmatrix} 0 & -K_{1,2} & \cdots & -K_{1,N-1} & -K_{1,N} \\ -K_{2,1} & 0 & \cdots & -K_{2,N-1} & -K_{2,N} \\ \vdots & \vdots & \ddots & \vdots & \vdots \\ -K_{N-1,1} & -K_{N-1,2} & \cdots & 0 & -K_{N-1,N} \\ 1 & 0 & \cdots & 0 & 1 \end{bmatrix} \begin{bmatrix} \gamma_1 \\ \gamma_2 \\ \vdots \\ \gamma_{N-1} \\ \gamma_N \end{bmatrix} = \begin{bmatrix} -V_\infty 2\pi\cos(\beta_1) \\ -V_\infty 2\pi\cos(\beta_2) \\ \vdots \\ -V_\infty 2\pi\cos(\beta_{N-1}) \\ 0 \end{bmatrix}$$

The total tangential velocity at each control points is [1]

$$V_{t,i} = V_\infty \sin(\beta_i) + \frac{\gamma}{2} - \sum_{\substack{j=1 \\ (j\neq 1)}}^{n} \frac{\lambda_j\, L_{i,j}}{2\pi} \tag{10}$$

where $L_{i,j}$ is the tangential velocity geometric integral of panel i relative to panel j. $L_{i,j}$ is evaluated like $I_{i,j}$ where

$$C = \sin(\phi_j - \phi_i)$$
$$D = -(y_i - Y_j)\cos\phi_i + (x_i - X_j)\sin\phi_i$$

The velocity at each panel is used to find the pressure coefficient as shown in Equation 6. The vortex panel method is sensitive to panel resolution and often produces definitively incorrect results. Through trial and error, the panel resolution may be tuned to produce accurate results.

2.3 Combined Source and Vortex Panel Method

Both the source and vortex panel methods have their limitations; the source panel method cannot predict lift, and the vortex panel method is sensitive to panel resolution. Combining the two methods produces accurate and reliable results. The combined source and vortex panel method uses the same source panel methodology of creating panels of sources that vary in strength from panel to panel, but vortex panels are also created but do not vary from panel to panel but are constant for the entire body. The normal velocity equation is [2]

$$V_{n,i} = V_\infty \cos(\beta_i) + \frac{\lambda_i}{2} + \sum_{\substack{j=1 \\ (j\neq i)}}^{n} \frac{\lambda_j\, I_{i,j}}{2\pi} - \sum_{\substack{j=1 \\ (j\neq i)}}^{n} \frac{\gamma_j\, K_{i,j}}{2\pi} = 0 \tag{11}$$

Like the vortex panel method, the Kutta condition must be applied at the trailing edge, but the vortex strength cannot be zero as it was previously. The Kutta condition is satisfied by setting the trailing edge panels' velocities equal. Adding the velocities is described by [2]

$$V_\infty \sin\beta_1 + \sum_{j=2}^{N} \frac{\lambda_j\, J_{1,j}}{2\pi} + \frac{1}{2}\gamma - \sum_{j=2}^{N} \frac{\gamma\, L_{1,j}}{2\pi} + V_\infty \sin\beta_N + \sum_{j=2}^{N-1} \frac{\lambda_j\, J_{N,j}}{2\pi} + \frac{1}{2}\gamma - \sum_{j=2}^{N-1} \frac{\gamma\, L_{N,j}}{2\pi} = 0 \tag{12}$$

Equation 11 and 12 create a system of equations in the following matrix form

$$\begin{bmatrix} \pi & I_{1,2} & \cdots & I_{1,N} & -(K_{1,2}+K_{1,3}+\cdots+K_{1,N}) \\ I_{2,1} & \pi & \cdots & I_{2,N} & -(K_{2,1}+K_{2,3}+\cdots+K_{2,N}) \\ \vdots & \vdots & \ddots & \vdots & \vdots \\ I_{N,1} & I_{N,2} & \cdots & \pi & -(K_{N,1}+K_{N,2}+\cdots+K_{N,N-1}) \\ J_{N,1} & J_{1,2}+J_{N,2} & \cdots & J_{1,N} & \begin{matrix} -\left(L_{1,2}+\cdots+L_{1,N}\right) \\ -\left(L_{N,1}+\cdots+L_{N,2}\right)+2\pi \end{matrix} \end{bmatrix} \begin{bmatrix} \lambda_1 \\ \lambda_2 \\ \vdots \\ \lambda_N \\ \gamma \end{bmatrix} = \begin{bmatrix} -V_\infty 2\pi\cos(\beta_1) \\ -V_\infty 2\pi\cos(\beta_2) \\ \vdots \\ -V_\infty 2\pi\cos(\beta_N) \\ -V_\infty 2\pi(\sin\beta_1+\sin\beta_N) \end{bmatrix}$$

The matrix is solved for the source panel strengths λ and the vortex strength γ. The total tangential velocity at each control points is [2]

$$V_{t,i} = V_\infty \sin\beta_i + \sum_{\substack{j=1 \\ j\neq i}}^{N} \frac{\lambda_j J_{i,j}}{2\pi} + \frac{1}{2}\gamma - \sum_{\substack{j=1 \\ j\neq i}}^{N} \frac{\gamma L_{i,j}}{2\pi} \tag{13}$$

The velocity at each panel is used to find the pressure coefficient as shown in Equation 6. The combined source panel method is not sensitive to panel resolution and produces accurate estimations of lift and pressure drag.

3 Results and Discussion

A Python script was developed to handle an input of boundary points, angle of attack, and freestream velocity to create panels, solve for the pressure coefficients, and calculate lift. The code is found in the Appendix. The script was used to solve for the lift of the NACA 0012 airfoil for angles of attack from -5 to 20 degrees and a comparison to experimental data is shown in Figure 2.

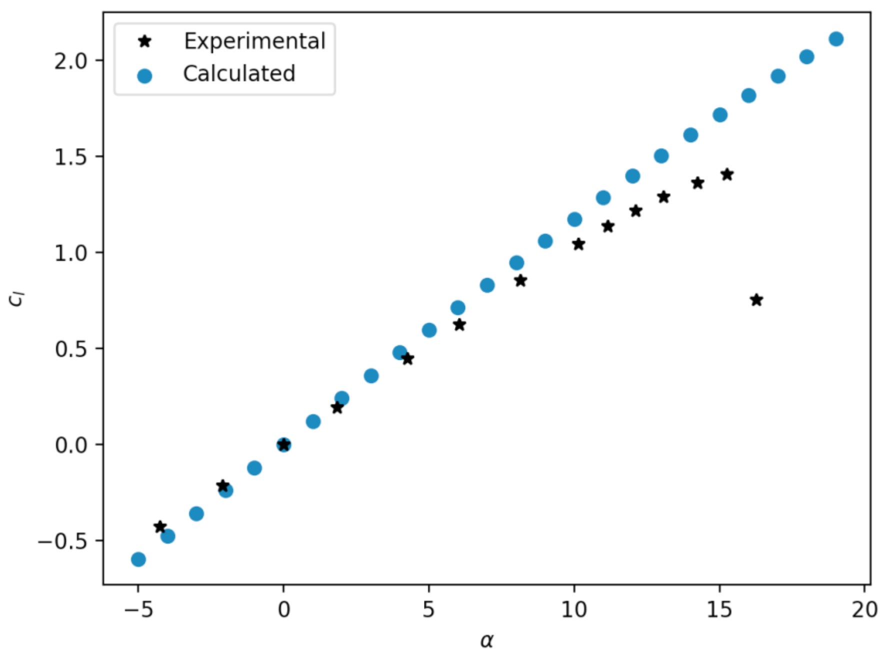

Figure 2: Experimental [3] and calculated c_l vs α for the NACA 0012 airfoil.

Figure 2 shows a strong correlation between the experimental and calculated data at small angles of attack. This result is as expected because the numerical panel method does not consider viscous effects. Flow separation is not accounted for at high angles of attack. Notice that the calculated always has more lift than the experimental, this further validates the prediction. It is also noted that both sets of data show a lift coefficient of zero at zero angle of attack. This result is expected for a symmetric airfoil.

The NACA 2412 cambered airfoil was also analyzed using the script. The lift was solved for -20 to 20 degrees angle of attack. A comparison is shown in Figure 3.

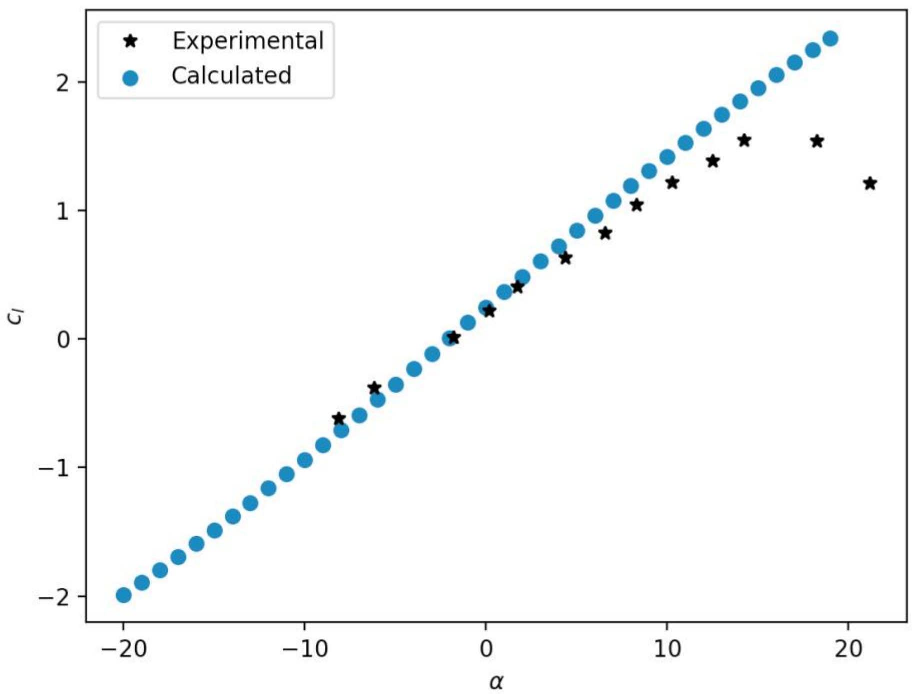

Figure 3: Experimental [1] and calculated c_l vs α for the NACA 0012 airfoil.

Figure 3 shows a strong correlation between the experimental and calculated data at small angles of attack. Different from the NACA 0012, the NACA 2412 has a non-zero lift at zero angle of attack because of the camber. Based on the raw calculated data, the angle of attack of zero lift is at -2.13 degrees.

Figure 4 shows the pressure distribution as a function of x/c for the zero-lift angle of attack, a 0 degree angle of attack, and 10 a degree angle of attack.

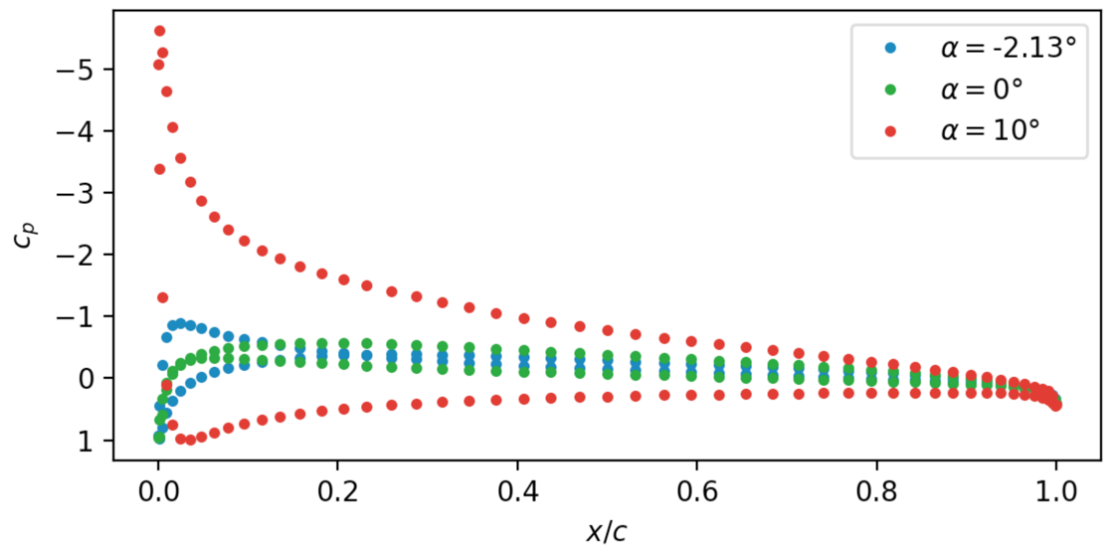

Figure 4: NACA 2412 pressure distribution at -2.13, 0, and 10 degree angle of attacks.

Figure 4 shows that the area under the curve increases as the angle of attack increases. This result is expected because the area under the curve determines lift. In general, and at small angles, more angle of attack produces more lift. It also shows that for a cambered airfoil, the 0 degree angle of attack is lifting. Figure 5 shows the pressure distribution around the body at the various angles of attack. Notice that the higher angles of attack have high pressure on the bottom of the airfoil and low pressure around the top of the airfoil.

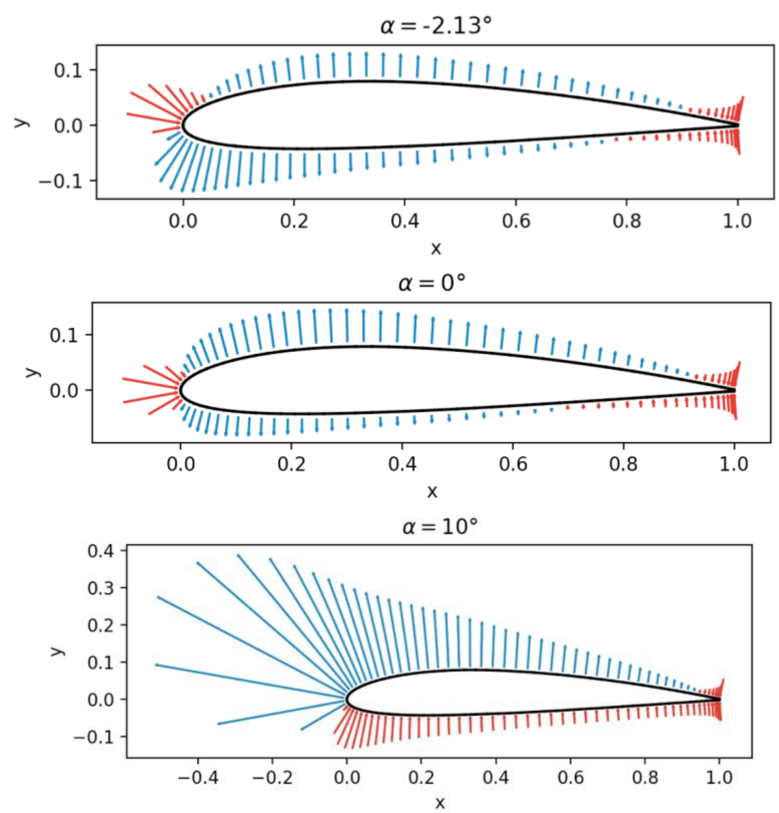

Figure 5: Scaled pressure vectors on the NACA 2412 at various angles of attack.

The combined source and vortex panel method produces accurate models of pressure over an aerodynamic body. The models can be used to analyze different body shapes to maximize lift at low angles of attack. Numerical panel methods are still used in modern aerodynamic analysis.

4 References

[1] J. D. Anderson, Fundamentals of Aerodynamics, New York: McGraw-Hill Education, 2016.

[2] JoshTheEngineer, "Source/Vortex Panel Method: System of Equations," 10 May 2020. [Online]. Available: https://www.youtube.com/watch?v=bc_pkKGEypU&t=450s. [Accessed 8 December 2021].

[3] C. L. Ladson, "Effects of Independent Variation of Mach and Reynolds Numbers on the Low-Speed Aerodynamic Characteristics of the NACA 0012 Airfoil Section," October 1988. [Online]. Available: https://ntrs.nasa.gov/api/citations/19880019495/downloads/19880019495.pdf. [Accessed 8 December 2021].